

# NASA TECHNICAL NOTE



NASA TN D-8071 c.1

NASA TN D-8071

2. u/u

LOAN COPY: RE  
AFWL TECHNICAL  
KIRTLAND AFB



## COMPARATIVE THERMAL FATIGUE RESISTANCES OF TWENTY-SIX NICKEL- AND COBALT-BASE ALLOYS

*Peter T. Bizon and David A. Spera*

*Lewis Research Center*

*Cleveland, Ohio 44135*



NATIONAL AERONAUTICS AND SPACE ADMINISTRATION • WASHINGTON, D. C. • OCTOBER 1975



0133691

1. Report No. NASA TN D-8071	2. Government Accession No.	3. Recd.
4. Title and Subtitle <b>COMPARATIVE THERMAL FATIGUE RESISTANCES OF TWENTY-SIX NICKEL- AND COBALT-BASE ALLOYS</b>		5. Report Date <b>October 1975</b>
7. Author(s) <b>Peter T. Bizon and David A. Spera</b>		6. Performing Organization Code
9. Performing Organization Name and Address <b>Lewis Research Center National Aeronautics and Space Administration Cleveland, Ohio 44135</b>		8. Performing Organization Report No. <b>E-8305</b>
12. Sponsoring Agency Name and Address <b>National Aeronautics and Space Administration Washington, D. C. 20546</b>		10. Work Unit No. <b>505-01</b>
15. Supplementary Notes		11. Contract or Grant No.
16. Abstract  The comparative thermal fatigue resistances of 26 nickel- and cobalt-base alloys were determined from fluidized bed tests. Cycles to cracking differed by almost three orders of magnitude for these materials with directional solidification and surface protection of definite benefit. The alloy-coating combination with the highest thermal fatigue resistance was directionally solidified NASA TAZ-8A with an RT-XP coating. Its oxidation resistance also was excellent, showing almost no weight change after 15 000 fluidized bed cycles.		13. Type of Report and Period Covered <b>Technical Note</b>
17. Key Words (Suggested by Author(s))  Thermal fatigue      Cobalt alloys Oxidation              Fluidized bed Coatings                Superalloys Nickel alloys            Mechanical properties		14. Sponsoring Agency Code
18. Distribution Statement <b>Unclassified - unlimited STAR Category 39 (rev.)</b>		
19. Security Classif. (of this report) <b>Unclassified</b>	20. Security Classif. (of this page) <b>Unclassified</b>	21. No. of Pages <b>39</b>
		22. Price* <b>\$3.75</b>

# COMPARATIVE THERMAL FATIGUE RESISTANCES OF TWENTY-SIX NICKEL- AND COBALT-BASE ALLOYS

by Peter T. Bizon and David A. Spera

Lewis Research Center

## SUMMARY

This experimental program used the fluidized bed heating and cooling technique to compare the measured thermal fatigue resistances of 26 nickel- and cobalt-base alloys. These included nineteen cast and two wrought nickel-base alloys, and five cast cobalt-base alloys. Five of the nickel-base alloys had directionally solidified polycrystalline grain structures. Three diffusion coatings and one vapor-deposited overlay coating were also included in this investigation.

The same specimen geometry (double-wedge) and test conditions were used to evaluate all materials. Groups of specimens were thermally cycled between fluidized beds operating at  $1088^{\circ}$  and  $316^{\circ}$  C ( $1990^{\circ}$  and  $600^{\circ}$  F), with a 3-minute immersion time in each bed. Some materials were also tested with both bed temperatures raised  $42^{\circ}$  C ( $75^{\circ}$  F). These tests were performed at the Illinois Institute of Technology Research Institute under contract to NASA Lewis Research Center. The number of cycles required to initiate a crack in the edge of a specimen was the measure of its thermal fatigue resistance. In addition, oxidation and some mechanical and physical property data were compared at selected temperatures.

Thermal fatigue resistances under the same test conditions ranged from less than 25 to 12 500 cycles for the 35 combinations of alloys and coatings studied. Alloys with a directionally solidified polycrystalline grain structure had the longest thermal fatigue lives. In all cases, coatings improved the thermal fatigue resistance of the substrate alloy.

The alloy-coating combination with the highest resistance to thermal fatigue was directionally solidified NASA TAZ-8A with a RT-XP coating. Its thermal fatigue life was almost twice that of the next best alloy-coating combination. In addition, directionally solidified TAZ-8A + RT-XP coat had excellent oxidation resistance, showing almost no weight change after 15 000 cycles (750 hr of heating time).

## INTRODUCTION

Thermal fatigue is a potential mode of failure in any component that is exposed to fluctuating temperatures. Thermal fatigue can be defined simply as the cracking of a material by cyclic temperature changes which induce cyclic stresses. Thermal fatigue resistance is one of the major criteria which should be considered when selecting an alloy for a fluctuating temperature application. As an example, thermal fatigue cracking is currently the predominant failure mode for aircraft gas turbine blades.

Thermal fatigue resistance is not a basic material property such as tensile strength, density, and so forth, but a structural response. It is dependent upon a complex combination of many factors including component geometry, temperature cycle, heat-transfer rates, oxidation resistance, and physical and mechanical properties of the material (such as modulus of elasticity, coefficient of thermal expansion, strength, ductility, etc.). Hence, the number of temperature cycles required to cause thermal fatigue cracking depends not only on the alloy but also on the specimen geometry and test conditions. In this investigation, the term "thermal fatigue resistance" is used in a comparative, rather than absolute, sense. Alloys are compared to one another, all having been tested under the same test conditions using the same specimen geometry.

The primary objective of this investigation was to determine the comparative thermal fatigue resistance of a large number of nickel- and cobalt-base alloys. A secondary objective was to determine the effects of directional solidification and several coatings on both the thermal fatigue and oxidation resistance of some of these alloys. The alloys selected include those used or proposed for use in the hot-test sections of advanced aircraft gas turbines.

Nineteen cast nickel-base alloys, five cast cobalt-base alloys, and two wrought nickel-base alloys were included in this study. Five of the nickel-base alloys had a directionally solidified polycrystalline grain structure. Three diffusion coatings and one vapor-deposited overlay coating were also included in this investigation. This provided a total of 35 combinations of composition, grain structure, and surface protection. Specimens were in the form of prismatic bars with double-wedge cross sections.

The thermal fatigue tests were carried out in a fluidized bed facility that was designed, built, and operated by the Illinois Institute of Technology Research Institute

(IITRI) under contract to NASA Lewis Research Center. Fluidized beds were first used for rapidly heating and cooling thermal fatigue specimens by E. Glenny and his coworkers at the National Gas Turbine Establishment in England in 1958 (ref. 1). Since that time, fluidized bed cycling has become widely used for evaluating the thermal fatigue behavior of both alloys and components (refs. 2 to 7).

Test conditions for the thermal fatigue evaluation were selected to represent advanced gas turbine engines and were, therefore, more severe than present use conditions for these alloys. All materials were evaluated using bed temperatures of 1088° and 316° C (1990° and 600° F). The effect of raising both bed temperatures 42° C (75° F) was also evaluated for some of the materials. Immersion time in each bed was always 3 minutes. In addition to thermal fatigue resistance, some mechanical and physical properties of the alloys were also compared at selected temperatures. The conventional mechanical property tests for the materials included in this investigation were conducted at the Lewis Research Center.

This investigation is part of a program of studies of failure mechanisms and life prediction of turbine components being performed by the Lewis Research Center. An overview of this program is given in reference 8 together with a bibliography of NASA Lewis publications on fatigue, oxidation and coatings, and turbine engine alloys. References 9 to 14 are earlier reports which contain initial data relative to the thermal fatigue tests described herein.

This work was conducted in the U. S. customary system of units except for the weight measurements. Conversion to International System of Units (SI) was made for reporting purposes only.

## MATERIALS AND TEST SPECIMENS

### Alloys

The 35 combinations of composition, grain structure, and surface protection which were studied in this program are listed in table I. Table II lists the compositions of the alloys (chemical analyses of heats used for test specimens) along with the various heat treatments applied to them. Selected physical properties (from handbooks) and mechanical properties (measured) are given in tables III and IV, respectively.

A new alloy included in this investigation is directionally solidified NASA TAZ-8A. In an earlier investigation (ref. 11) the random polycrystalline form of this

alloy was found to have the highest resistance to thermal fatigue among 14 uncoated alloys. This indicated that directional solidification and/or coating of TAZ-8A might produce a material with even better thermal fatigue resistance. Specimens with directional polycrystalline structure were then cast both at the Lewis Research Center and commercially for evaluation in this investigation.

### Surface Protection

Brief descriptions of the four protective coatings used in this study are as follows:

- (1) Jocoat -- a commercial silicon-modified nickel aluminide coating (Pratt and Whitney Aircraft proprietary process specified as PWA 47)
- (2) RT-1A -- a commercial chromium-aluminum duplex coating (Chromalloy American Corporation Research and Technology Division proprietary process similar to specification PWA 32 but with a lower process temperature)
- (3) RT-XP -- a coating containing an aluminide with a case depth of about 70  $\mu\text{m}$  (2.7 mils) (Chromalloy American Corporation Research and Technology Division proprietary process)
- (4) NiCrAlY -- a commercial Ni-15.2Cr-12Al-0.33Y electron-beam vapor-deposited overlay coating about 135  $\mu\text{m}$  (5.3 mils) thick (Pratt and Whitney Aircraft proprietary process specified as PWA 267)

### Test Specimens and Holding Fixtures

In this study two types of specimen configurations (fig. 1) were used -- wedge-shaped prismatic bars and round cross-sectional tensile bars. Figure 1(a) shows the wedge designs used for the thermal fatigue and oxidation tests. Although three designs of the double-wedge shape were used for the thermal fatigue tests, they differed only in the provision made for fastening them in the holding fixture. No consistent differences have been observed in the results of tests using the end grooves (design A) or holes (designs B and C) for fastening. Figure 2 shows groups of specimens in their respective holding fixtures. The outer two specimens were always dummy test specimens. The holding fixture using holes (fig. 2(b)) is preferred for tests at higher temperatures because of the lower mass of the fixture and

because the supporting rods are not exposed to as great an extent to the high temperatures.

Transient temperatures in some of the alloys were measured using instrumented specimens. These specimens were fitted with five embedded thermocouples at the midspan located as shown in figure 3. The ISA type K (Chromel-Alumel) thermocouples were magnesium oxide insulated and Inconel 600 sheathed with an outside sheath diameter of 0.5 mm (0.02 in.). The thermocouples were mounted in grooves milled in the surface of the specimen. The grooves were 0.56 mm (0.022 in.) wide and 0.5 mm (0.02 in.) deep. The thermocouples were secured in place by using an air-setting two-part Allen P-1 ceramic cement cured at 316° C (600° F).

Other oxidation or weight change tests were conducted with single-wedge specimens of design D shown in figure 1(a). This design has been used for some time to evaluate alloys in high-velocity burner rigs at the Lewis Research Center (ref. 15). This single-wedge design is recommended for future thermal fatigue studies. This is because the double-wedge does not always give additional data as was originally hoped. Actually, cracking on one edge of a specimen may delay crack initiation of the other edge.

Figure 1(b) presents typical designs for specimens used to measure conventional tensile and stress-rupture properties. Designs E and F are similar except that design F has flat grips so that it can be fabricated from 0.635 cm (0.25 in.) plate. Design F was used only for the TD NiCr tests. This was the thickest plate available in this alloy. The only essential difference between design G and designs E and F is the longer gage length of the design G specimens.

All cast specimens were cast-to-size. For the random polycrystalline specimens, inoculated molds were used to produce fine grain structures. Typical surface grain size at the test sections was about 1.6 mm (0.06 in.) diameter. The directionally solidified polycrystalline specimens were made using a controlled solidification process similar to that detailed in reference 16. Only directionally solidified specimens with no grain boundaries intercepting the leading edge were tested. Specimens of the two wrought alloys (U 700 and TD NiCr) were machined with the specimen axis parallel to the rolling or extrusion direction. All specimens were given radiographic, fluorescent penetrant, and visual inspections before testing.

## FLUIDIZED BED FACILITY AND TEST PROCEDURE

### Fluidized Bed Facility

Figure 4 is a drawing showing a cutaway view of the fluidized bed test facility (ref. 17) used. Both heating and cooling beds consist of retorts filled with 300- to 540- $\mu\text{m}$ - (0.012- to 0.021-in.-) diameter alumina particles through which air is pumped. Adjustment of the airflow allows the particles to develop a churning, circulating action -- hence, the name "fluidized". The large number of particles in the beds and their "fluid" action promote uniform, high heat transfer rates. A group of specimens in the holding fixture was cycled between the beds by means of an automatically controlled transfer mechanism operated by pneumatic cylinders.

The heating bed is 23 cm (9 in.) in diameter, contains 1100 N (250 lb) of alumina, and has a power input of 55 kW. Its airflow rate is 17 m<sup>3</sup>/hr (600 cu ft/hr). The cooling bed is 36 cm (14 in.) in diameter, and contains 1500 N (340 lb) of alumina. It uses 12 kW of power and has an airflow of 60 m<sup>3</sup>/hr (2100 cu ft/hr).

### Thermal Fatigue Test Procedure

Comparative thermal fatigue resistance was determined experimentally by simultaneously testing different materials of the same geometry and comparing the number of cycles required to initiate the first crack. A group of up to 18 double-wedge shaped specimens was alternately heated for 3 minutes and then cooled for 3 minutes. All materials were tested with the heating bed temperature held at 1088<sup>o</sup> C (1990<sup>o</sup> F) and the cooling bed temperature at 316<sup>o</sup> C (600<sup>o</sup> F). The effect on some of the materials of raising both bed temperatures 42<sup>o</sup> C (75<sup>o</sup> F) was also evaluated.

Prior to testing and periodically thereafter, both edges of each specimen were visually examined using a microscope with a magnification of 30 times. Only the surfaces within  $\pm 3.8$  cm ( $\pm 1.5$  in.) of midlength were examined for cracks. Inspections were made according to a schedule such as 25, 50, 100, 200, 300, 500, 700, 1000, and so forth cycles, with the inspection intervals lengthening as the number of cycles applied increased. Inspection intervals for any series never exceeded 1000 cycles including the series which was tested the longest (15 000 cycles). The number of cycles to crack initiation was taken as the average of the number of cycles



at the last inspection without cracks and the number of cycles at the first inspection with a crack.

## RESULTS AND DISCUSSION

### Transient Temperatures

A typical transient temperature distribution for one heating and cooling fluidized bed cycle is given in figure 3. While these results are for directionally solidified TAZ-8A alloy at bed temperatures of  $1088^{\circ}\text{C}$  and  $316^{\circ}\text{C}$  ( $1990^{\circ}\text{F}$  and  $600^{\circ}\text{F}$ ), they are also typical of the transient temperature distribution for other alloys tested at these bed temperatures. Figure 3 shows that the maximum temperature difference within the specimens occurred about 0.1 to 0.2 minute after the start of heating and was approximately  $310^{\circ}\text{C}$  ( $560^{\circ}\text{F}$ ). During the cooling cycle, the maximum temperature difference occurred between 0.2 and 0.3 minute after the start of cooling and was approximately  $230^{\circ}\text{C}$  ( $415^{\circ}\text{F}$ ). This indicates that the average heat transfer coefficient during heating is higher than during cooling. This is consistent with measured values given in reference 1. This figure also shows that the specimens did not quite reach the bed temperature after 3 minutes immersion. The maximum metal temperature was about  $14^{\circ}\text{C}$  ( $25^{\circ}\text{F}$ ) less than the heating bed temperature and the minimum metal temperature was about  $33^{\circ}\text{C}$  ( $60^{\circ}\text{F}$ ) higher than the cooling bed temperature. Since the test conditions in this study were selected to represent those to be encountered in advanced gas turbine engine blades, the maximum metal temperature exceeded the use temperature for which many of the materials were designed. However, to obtain comparative thermal fatigue resistances for all materials, a uniform thermal cycle was necessary.

### Thermal Fatigue

The numbers of cycles required to initiate cracks in the 35 combinations of alloys and coatings are listed in table V and plotted in figure 5. All results except where noted are for the 0.635-cm (0.25-in.) radius edge only. For the same specimen geometry and test conditions, the lives varied from less than 25 cycles to 12 500 cycles. Reproducibility of test data was generally good.

The class of materials having the longest thermal fatigue lives was found to be cast alloys with directionally solidified polycrystalline grain structures. The alloy-

coating combination with the highest thermal fatigue resistance was directionally solidified NASA TAZ-8A with an RT-XP coating. Its thermal fatigue life was almost double that of the next best alloy-coating combination, directionally solidified Mar-M 200 with the overlay coating NiCrAlY. The application of a coating in all cases improved the thermal fatigue resistance of the substrate alloy.

Of all the random polycrystalline alloys tested, hafnium-modified B 1900 with Jocoat had the highest thermal fatigue resistance (1480 cycles). However, of the nineteen uncoated random polycrystalline alloys tested, NASA TAZ-8A again had the highest thermal fatigue resistance (700 cycles).

Some of the materials were also tested when both the maximum and minimum temperatures of the fluidized beds were raised by  $42^{\circ}\text{C}$  ( $75^{\circ}\text{F}$ ). A comparison of the thermal fatigue resistances for materials tested at both bed temperature conditions is presented in figure 6. These results are also plotted in the order of decreasing thermal fatigue life of the  $1088^{\circ}\text{C}$  and  $316^{\circ}\text{C}$  ( $1990^{\circ}\text{F}$  and  $600^{\circ}\text{F}$ ) tests. Superimposing the results of the  $1130^{\circ}\text{C}$  and  $357^{\circ}\text{C}$  ( $2065^{\circ}\text{F}$  and  $675^{\circ}\text{F}$ ) tests on this figure reveals that raising the bed temperatures resulted in only minor changes in comparative thermal fatigue resistance.

An interesting observation was made regarding the two alloys NASA TAZ-8A and M 22. Reference to table II shows the similarity of the compositions (considering the refractory elements as a group) of these two alloys. It is observed from figure 5, however, that their thermal fatigue resistances differ widely. Further study of these two alloys might identify the elements or phases which greatly affect thermal fatigue resistance in nickel-base alloys and lead to a better understanding of the thermal fatigue process.

Photographs of specimens representing each of the 35 combinations of alloys and coatings after completion of cycling tests are shown in figure 7. Caution must be exercised in comparing these photographs because of the wide range of cycles (470 to 14 000) at which they were taken. It is interesting to note the type of cracks in the two materials having the highest thermal fatigue resistance. Both directionally solidified NASA TAZ-8A with the RT-XP coating (fig. 7(a)) and directionally solidified Mar-M 200 with the NiCrAlY overlay (fig. 7(c)) have very tight cracks after 14,000 and 10,000 cycles respectively. In the uncoated condition the directionally solidified NASA TAZ-8A (also fig. 7(a)) still has relatively tight cracks after 6250 cycles while the cracks in directionally solidified Mar-M 200 (also fig. 7(c)) have

opened up markedly after only 4000 cycles.

In some materials, longitudinal cracks originated at the holding grooves or holes in the specimens. For example, as can be seen in figure 7(g), TD NiCr exhibited very large longitudinal cracks which started at the holding grooves. Thus, it is apparent that stress concentrations in nominally low-stress regions may cause unexpected cracks, particularly in anisotropic materials.

The superior resistance to thermal fatigue of directionally solidified polycrystalline alloys may be attributed to two factors: lower modulus of elasticity and an absence of transverse grain boundaries. First, as can be noted from table III, where data are available the modulus of elasticity along the growth direction is lower than that of the same alloy in the random polycrystalline form. The modulus varies from about two-thirds at room temperature to about one-half at  $1093^{\circ}\text{C}$  ( $2000^{\circ}\text{F}$ ). Also, as can be seen in table III, thermal expansion and conductivity of the alloys are independent of the structure, being dependent only on the composition. Therefore, in tests using the same geometry and identical test conditions, a specimen of a directionally solidified polycrystalline alloy is subjected to significantly lower cyclic stresses than one of the same alloy in a random polycrystalline structure although both have equal cyclic strains.

A second characteristic of directionally solidified alloys which aids their thermal fatigue resistance is the grain structure itself. The directional casting process produced long columnar grains so that there were no grain boundaries intercepting the leading edge. This removed locations which might serve as crack nuclei. The beneficial effect of the elimination of transverse grain boundaries can be seen by noting crack propagation in directional alloys. If a crack did initiate, the directional grains would tend to be barriers to propagation. This can be seen in both figures 8 and 9. Figure 8 shows photographs of the directionally solidified alloys before testing, at an intermediate stage of testing (in some cases), and after testing at bed temperatures of  $1130^{\circ}\text{C}$  and  $357^{\circ}\text{C}$  ( $2065^{\circ}\text{F}$  and  $675^{\circ}\text{F}$ ). Figure 8(e) shows a macrophotograph of directionally solidified Mar-M 200 before and after testing for 2400 cycles. Note how the crack had turned to grow along the longitudinal grain direction. The blunting of a crack by the directional grains can also be seen by referring to figure 9 (ref. 9). In this case the photomicrographs of directionally solidified NASA WAZ-20 alloy show that the surface crack was sufficiently blunted by the grain boundary to retard crack growth.

## Oxidation

The materials exhibited a wide variation in oxidation resistance. This may be seen from figures 7 and 8 which show photographs of some alloys before and after testing. In general, a coating or vapor-deposited overlay on a alloy gave a greatly reduced weight loss. Without surface protection, the directionally solidified alloys oxidized much faster than the same compositions in the random polycrystalline form.

Weight changes in the NASA TAZ-8A specimens during  $1088^{\circ}$  and  $316^{\circ}$  C ( $1990^{\circ}$  and  $600^{\circ}$  F) tests are shown in figure 10. Both directionally solidified polycrystalline and random polycrystalline grain structures were tested (1) uncoated, (2) with the RT-XP coat, and (3) with a NiCrAlY overlay coating. Specimen configurations were of design D of figure 1(a). Each specimen was weighed initially and at subsequent inspection periods during testing using an analytical balance measuring to within 1 mg. Figure 10 immediately shows the higher weight loss of the uncoated directionally solidified alloy over that of the uncoated random polycrystalline alloy. Specimens of both structures which had the overlay applied had about the same weight loss. This was considerably less than the uncoated directionally solidified form. Specimens of both structures of NASA TAZ-8A with the RT-XP coating exhibited almost no weight change even after 15 000 cycles of testing. Therefore, directionally solidified NASA TAZ-8A with the RT-XP coating which has already been noted to have excellent thermal fatigue resistance, also is seen to have excellent oxidation resistance.

Figure 11 shows a comparison of the weight changes for directionally solidified TAZ-8A and Mar-M 200, the alloy with the next highest thermal fatigue resistance. All data are for double-wedge specimens (designs B and C of figure 1(a)) tested with bed temperatures of  $1088^{\circ}$  and  $316^{\circ}$  C ( $1990^{\circ}$  and  $600^{\circ}$  F). Results are presented for both alloys without a coating and with the NiCrAlY overlay coating. In addition, data for TAZ-8A with the RT-XP coat are also presented. In figure 11, the comparison of both alloys in the uncoated condition shows the much higher weight loss of Mar-M 200 over that of TAZ-8A. The effect of applying coatings to both alloys is to greatly improve oxidation resistance.

## SUMMARY OF RESULTS

The comparative thermal fatigue resistances of 26 nickel- and cobalt-base alloys

were determined using the fluidized-bed technique. A total of 35 combinations of alloys and surface coatings were studied. All materials were evaluated by thermally cycling double-wedge specimens between two fluidized bed furnaces maintained at 1088° and 316° C (1990° and 600° F). Some materials were also exposed to bed temperatures of 1130° and 357° C (2065° and 675° F). Immersion times were 3 minutes in both the high and low temperature beds. Thermal fatigue resistance was based on the number of cycles required to initiate a crack. The major results obtained are as follows:

1. Thermal fatigue lives under identical test conditions ranged from less than 25 to 12 500 cycles among the 35 combinations of alloys and coatings.
2. The class of alloys having the longest thermal fatigue lives were cast alloys with directionally solidified polycrystalline grain structures.
3. The alloy-coating combination with the highest thermal fatigue resistance was directionally solidified NASA TAZ-8A with an RT-XP coating (coating containing an aluminide of Chromalloy American Corporation). Its thermal fatigue life was almost twice that of the next best alloy-coating combination. Its oxidation resistance was also excellent, showing almost no weight change after 15 000 cycles. Of the nineteen uncoated random polycrystalline alloys tested, NASA TAZ-8A had the highest thermal fatigue resistance.
4. The four coatings investigated always increased the thermal fatigue resistance of the substrate alloy.
5. Uncoated directionally solidified materials generally oxidized more rapidly than the same alloy in the random polycrystalline form. Application of diffusion coatings or a vapor-deposited overlay coating on the directionally solidified alloys greatly reduced weight loss.

Lewis Research Center,  
National Aeronautics and Space Administration,  
Cleveland, Ohio, May 16, 1975,  
505-01.

## REFERENCES

1. Glenny, E.; Northwood, J. E.; Shaw, S. W. K.; and Taylor, T. A.: A Technique for Thermal-Shock and Thermal-Fatigue Testing Based on the Use of Fluidized Solids. *J. Inst. Metals*, vol. 87, 1958-1959, pp. 294-302.
2. Glenny, E.; and Taylor, T. A.: A Study of the Thermal-Fatigue Behaviour of Metals. *J. Ins. Metals*, vol. 88, 1959-1960, pp. 449-461.
3. Franklin, A. W.; Heslop, J.; and Smith, R. A.: Some Metallurgical Factors Influencing the Thermal-Fatigue Resistance of Wrought Nickel-Chromium-Base High-Temperature Alloys. *J. Inst. Metals*, vol. 92, 1963-1964, pp. 313-321.
4. Howes, M. A. H.: Heat Checking in Die Casting Dies. *Die Casting Eng.*, vol. 13, 1969, p. 12.
5. Howes, M. A. H.; and Saperstein, Z. P.: The Thermal Fatigue of Copper-to-Steel Joints. *Welding J.*, vol. 48, Dec. 1969, pp. 543s-550s.
6. Rostoker, W.: Thermal Fatigue Resistance of Martensitic Steels. *J. Mat.*, vol. 4, no. 1, Mar. 1969, pp. 117-144.
7. Mowbray, D. F.; Woodford, D. A.; and Brandt, D. E.: Thermal Fatigue Characterization of Cast Cobalt and Nickel-Base Superalloys. Symposium on Fatigue at Elevated Temperatures. STP 520, American Society for Testing and Materials, 1973, 416-426.
8. Spera, David A.; and Grisaffe, Salvatore J.: Life Prediction of Turbine Components: On-Going Studies at the NASA Lewis Research Center. NASA TM X-2664, 1973.
9. Bizon, Peter T.; and Oldrieve, Robert E.: Thermal Fatigue Resistance of NASA WAZ-20 Alloy With Three Commercial Coatings. NASA TM X-3168, 1975.
10. Spera, David A.; Howes, Maurice A. H.; Bizon, Peter T.: Thermal Fatigue Resistance of 15 High-Temperature Alloys Determined by the Fluidized-Bed Technique. Presented at American Society for Metals, Western Metal and Tool Exposition Conf., Los Angeles, Calif., Mar. 8-11, 1971.
11. Howes, Maurice A. H.: Thermal Fatigue Data on 15 Nickel- and Cobalt-Base Alloys. (IITRI-B6078-38, IIT Research Institute; NAS3-9411.), NASA CR-72738, 1970.

12. Howes, Maurice A. H.: Additional Thermal Fatigue Data on Nickel- and Cobalt-Base Superalloys. (IITRI-B6107-34-Pt-1, IIT Research Institute; NAS3-14311.), NASA CR-121211, 1973.
13. Howes, M. A. H.: Additional Thermal Fatigue Data on Nickel and Cobalt-Base Superalloys. (IITRI-B6107-34-Pt-2, IIT Research Institute; NAS3-14311.), NASA CR-121212, 1973.
14. Howes, M. A. H.: Thermal Fatigue and Oxidation Data on TAZ-8A, Mar-M 200, and Udimet 700 Superalloys. (IITRI-B6124-21, IIT Research Institute; NAS3-17787.), NASA CR-134775, 1975.
15. Johnston, James R.; and Ashbrook, Richard L.: Oxidation and Thermal Fatigue Cracking of Nickel- and Cobalt-Base Alloys in a High Velocity Gas Stream. NASA TN D-5376, 1969.
16. Freche, John C.; Waters, William J.; and Ashbrook, Richard L.: Application of Directional Solidification to a NASA Nickel-Base Alloy (TAZ-8B) NASA TN D-4390, 1968.
17. Howes, M. A. H.: Evaluation of Thermal Fatigue Resistance of Metals Using the Fluidized Bed Technique. Symposium on Fatigue at Elevated Temperatures. STP 520, American Society for Testing and Materials, 1973, 242-254.

TABLE I. - ALLOYS AND CONDITIONS

[Coated and uncoated specimens purchased from vendors except where noted. DS indicates that the alloy was cast with a directionally solidified grain structure.]

NASA TAZ-8A DS + RT-XP coat	<sup>b</sup> B 1900 + Hf + Jocoat
NASA TAZ-8A DS + NiCrAlY overlay	B 1900 + Jocoat
<sup>a</sup> NASA TAZ-8A DS	B 1900
NASA TAZ-8A	U 700 cast
<sup>b</sup> NX 188 DS + RT-1A coat	U 700 wrought
<sup>b</sup> NX 188 DS	X 40
<sup>b</sup> NX 188 + RT-1A coat	IN 162
<sup>b</sup> NX 188	TD NiCr
Mar-M 200 DS + NiCrAlY overlay	IN 713C
Mar-M 200 DS	Mar-M 509
Mar-M 200 + Jocoat	NASA VI-A
Mar-M 200	<sup>c</sup> René 80
IN 100 DS + Jocoat	IN 738
IN 100 DS	<sup>d</sup> RBH
IN 100 + Jocoat	Mar-M 302
IN 100	WI 52
	M 22
<sup>a</sup> NASA WAZ-20 DS + Jocoat	
<sup>a</sup> NASA WAZ-20 + Jocoat	

<sup>a</sup>Specimens cast at NASA Lewis Research Center.

<sup>b</sup>Specimens with and without coatings supplied by Pratt & Whitney Aircraft Corp.

<sup>c</sup>Specimens supplied by General Electric Corp.

<sup>d</sup>Specimens supplied by Cabot Corp.



TABLE II. - COMPOSITION AND HEAT TREATMENT

[DS indicates that the alloy was cast with a directionally solidified grain structure.]

Alloy	Heat number	Analyzed composition, wt. %													Heat treatment
		C	Mn	Si	Cr	Ni	Co	Mo	W	Al	Ti	Zr	B	Other	
NASA TAZ-8A DS	T-24	0.10	-----	-----	5.85	Bal	-----	5.41	3.90	6.40	----	0.52	39 ppm	7.93Ta, 2.44Cb	As cast
Mar-M 200 DS	KD 2012	0.15	<0.02	0.080	9.20	Bal	10.25	-----	12.55	5.05	2.13	0.048	0.017	0.36Fe, 0.96Cb, <0.01V	816°C (1500°F) for 50 hr
NX 188 DS	EXF 1655	0.033	-----	-----	-----	-----	-----	18.03	-----	8.13	-----	-----	-----	-----	As cast
IN 100 DS	KJ 2206	0.17	<0.02	0.11	10.30	Bal	15.10	2.96	-----	5.45	4.76	0.084	0.016	0.21Fe, 0.97V	1149°C (2100°F) for 2 hr; 927°C (1700°F) for 16 hr
NASA WAZ-20 DS	-----	0.17	-----	-----	-----	Bal	-----	-----	20.9	6.28	----	1.2	-----	-----	As cast
B 1900 + Hf	-----	0.09	0.003	0.06	8.13	Bal	10.19	5.90	0.04	5.96	0.98	0.04	0.009	4.3Ta, 0.06Fe, 1.64Hf	1080°C (1975°F) for 4 hr; 899°C (1650°F) for 10 hr
NASA TAZ-8A	67-640	0.01	-----	-----	6.20	Bal	-----	3.86	3.86	5.96	----	0.88	-----	8.01Ta, 2.44Cb	As cast
X 40	12C6412	0.48	<0.05	0.33	25.59	10.52	Bal	0.04	7.87	----	----	0.03	0.005	0.46Fe, 0.02N	760°C (1400°F) for 50 hr
B 1900	54V6335	0.10	0.10	<0.10	8.11	Bal	10.15	6.11	<0.10	6.09	0.98	0.08	0.013	4.28Ta, 0.16Fe, 4, 28V	843°C (1550°F) for 24 hr
IN 162	96317	0.10	0.01	0.04	10.03	Bal	0.03	4.05	2.03	6.35	0.93	0.11	0.018	1.97Ta, 0.17Fe, 0.88Cb	As cast
TD NiCr	1862	0.038	-----	-----	21.39	Bal	-----	-----	-----	-----	-----	-----	-----	2.5ThO <sub>2</sub> , 0.0005N, 0.006S	As cast
	2858	0.020	-----	-----	19.72	Bal	-----	-----	-----	-----	-----	-----	-----	1.9ThO <sub>2</sub> , 0.004N, 0.007S	As cast
IN 713C	65611	0.11	<0.10	<0.10	13.40	Bal	-----	4.50	-----	5.95	0.83	0.08	0.009	2.24Cb+Ta, 0.27Fe	As cast
Mar-M 509	T-3008	0.62	<0.1	<0.1	23.4	10.0	Bal	-----	6.95	-----	0.19	0.54	<0.01	3.46Ta, <0.1Fe	As cast
NX 188	EXF 1655	0.033	-----	-----	-----	-----	-----	18.03	-----	8.13	-----	-----	-----	-----	As cast
NASA VI-A	FB 5487	0.11	0.02	<0.10	5.86	Bal	7.24	2.11	5.96	5.27	0.95	0.10	0.021	9.03Ta, 0.32Re, 0.39Hf, 0.45Cb, 0.08Fe	899°C (1650°F) for 32 hr
NASA WAZ-20	-----	0.17	-----	-----	-----	Bal	-----	-----	20.9	6.28	----	1.2	-----	-----	As cast
René 80	101V9494	0.18	0.01	<0.10	14.0	Bal	9.91	4.00	3.84	3.11	4.90	0.03	0.014	0.18Fe, <1ppm Ag	1219°C (2225°F) for 2 hr; 1093°C (2000°F) for 4 hr; 1052°C (1925°F) for 4 hr; 843°C (1550°F) for 16 hr
IN 738	94V9529	0.17	0.01	0.11	15.98	Bal	8.37	1.81	2.49	3.52	3.39	0.11	0.012	1.95Ta, 0.14Fe, 0.87Cb	1121°C (2050°F) for 2 hr; 843°C (1550°F) for 24 hr
RBH	70-670-4	0.64	0.43	0.39	20.91	16.00	Bal	-----	5.46	0.33	0.24	0.16	-----	3.20Ta, 0.73Fe, 0.05La	As cast
Mar-M 302	T-272	0.88	<0.10	0.22	21.9	0.49	Bal	<0.1	9.89	----	----	0.24	<0.01	8.80Ta, 1.11Fe	1232°C (2250°F) for 8 hr; 816°C (1500°F) for 24 hr
U 700 cast	85V2416	0.08	<0.10	<0.10	14.24	Bal	14.87	4.18	-----	4.25	3.26	<0.01	0.012	0.30Fe	760°C (1400°F) for 16 hr
WI 52	59-682	0.46	0.21	0.28	20.86	0.23	Bal	<0.05	11.06	-----	-----	-----	-----	1.75Fe, 1.87Cb	As cast
IN 100	KJ 2206	0.17	<0.02	0.11	10.30	Bal	15.10	2.96	-----	5.45	4.76	0.084	0.016	0.21Fe, 0.97V	1149°C (2100°F) for 2 hr; 927°C (1700°F) for 16 hr
Mar-M 200	KD 2012	0.15	<0.02	0.080	9.20	Bal	10.25	-----	12.55	5.05	2.13	0.048	0.017	0.36Fe, 0.96Cb, <0.01V	816°C (1500°F) for 50 hr
U 700 wrought	6541	0.113	0.01	0.02	14.85	Bal	17.50	5.10	-----	4.55	3.45	<0.02	0.013	0.85Fe	1121°C (2050°F) for 4 hr; 843°C (1550°F) for 24 hr; 760°C (1400°F) for 16 hr
M 22	67-635	0.06	-----	-----	6.35	Bal	-----	1.96	11.37	6.24	----	0.65	-----	2.87Ta	As cast

TABLE III. - PHYSICAL PROPERTIES

[DS indicates that the alloy was cast with a directionally solidified grain structure.]

Alloy	Specific gravity at room temperature	Dynamic modulus of elasticity at room temperature		Mean coefficient of thermal expansion from room temperature to 93° C (200° F)		Thermal conductivity at 93° C (200° F)	
		N/m <sup>2</sup>	psi	$\frac{m}{m} \frac{1}{^{\circ}C}$	$\frac{in.}{in.} \frac{1}{^{\circ}F}$	$\frac{W}{(m)(K)}$	$\frac{Btu-in.}{(ft^2)(hr)(^{\circ}F)}$
NASA TAZ-8A DS	----	-----	-----	-----	-----	9.7	67
Mar-M 200 DS	8.55	<sup>a</sup> 146×10 <sup>9</sup>	<sup>a</sup> 21.2×10 <sup>6</sup>	11.5×10 <sup>-6</sup>	6.4×10 <sup>-6</sup>	14.4	100
NX 188 DS	8.22	<sup>a</sup> 134	<sup>a</sup> 19.5	11.2	6.2	18.7	130
IN 100 DS	----	-----	-----	13.0	7.2	11.5	80
NASA WAZ-20 DS	9.10	-----	-----	-----	-----	----	---
B 1900 + Hf	8.28	214	31.0	11.7	6.5	10.1	70
NASA TAZ-8A	8.65	-----	-----	-----	-----	9.7	67
X 40	8.60	226	32.8	12.1	6.7	13.5	94
B-1900	8.22	214	31.0	11.7	6.5	10.2	71
IN 162	8.08	197	28.5	12.2	6.8	----	---
TD NiCr	8.36	131	19.0	14.2	7.9	14.3	99
IN 713C	7.91	206	29.9	10.6	5.9	21.0	146
Mar-M 509	8.86	225	32.6	12.1	6.7	13.0	90
NX 188	----	210	30.5	11.2	6.2	18.7	130
NASA VI-A	8.75	-----	-----	11.2	6.2	----	---
NASA WAZ-20	8.94	-----	-----	-----	-----	----	---
René 80	8.17	206	29.9	12.2	6.8	10.7	74
IN 738	8.11	199	28.9	11.7	6.5	10.4	72
RBH	8.75	210	30.4	12.2	6.8	12.5	87
Mar-M 302	9.21	250	36.2	12.2	6.8	19.2	133
U 700 cast	7.91	223	32.4	13.3	7.4	19.7	137
WI 52	8.87	225	32.6	13.3	7.4	25.1	174
IN 100	7.75	215	31.2	13.0	7.2	11.5	80
Mar-M 200	8.41	205	29.8	11.5	6.4	14.4	100
U 700 wrought	7.91	223	32.4	13.3	7.4	19.7	137
M 22	8.63	197	28.6	12.4	6.9	----	---

<sup>a</sup>Along growth direction.

TABLE IV. - TENSILE AND STRESS-RUPTURE PROPERTIES

[Data from same heat as used for thermal fatigue tests except where noted. Test data are for fine grain structure where typical grain sizes were about 1.6 mm (0.63 in.) diameter. DS indicates that the alloy was cast with a directionally solidified grain structure.]

Alloy	Specimen design (see fig. 1(b))	Proportional limit at 760° C (1400° F) <sup>a</sup>				Ultimate tensile strength at 760° C (1400° F) <sup>a</sup>				Stress rupture at 982° C (1800° F)				Reduction of area, percent <sup>a</sup>			
		MN/m <sup>2</sup>	ksi	Percent of nominal 0.2 percent yield stress	Divided by room temperature specific gravity		MN/m <sup>2</sup>	ksi	Percent of nominal ultimate tensile strength	Divided by room temperature specific gravity		Stress		Life (nominal 100 hr)		760° C (1400° F) Tensile	982° C (1800° F) Rupture
					MN/m <sup>2</sup>	ksi				MN/m <sup>2</sup>	ksi	MN/m <sup>2</sup>	ksi	Hr	Percent of nominal life		
NASA TAZ-8A DS	G	896	130	93	---	----	1179	171	110	---	----	172	25	44, 148	96	5	30
Mar-M 200 DS <sup>b</sup>	---	869	126	---	102	14.7	1048	152	---	123	17.8	200	29	-----	---	6	--
NX 188 DS <sup>c</sup>	G	876	127	77	106	15.5	931	135	79	113	16.4	138	20	60, 55	58	4	25
IN 100 DS	E	841	122	---	---	----	1034	150	107	---	----	159	23	144, 164	154	16	62
NASA WAZ-20 DS <sup>c</sup>	G	703	102	96	78	11.2	855	124	104	95	13.6	172	25	43, 77	60	9	19
B 1900 + Hf <sup>c</sup>	G	703	102	88	84	12.3	945	137	92	115	16.5	169	24.5	66, 34	50	13	13
NASA TAZ-8A	E	1034	150	---	119	17.3	1200	174	134	138	20.1	124	18	89, 79	84	2	8
X 40	E	386	56	---	45	6.5	593	86	123	69	10.0	76	11	183, >105	183	20	33
B 1900	E	938	136	116	114	16.5	1089	158	114	133	19.2	172	25	99, 95	97	8	11
IN 162	E	896	130	106	111	16.1	1124	163	112	139	20.2	165	24	115, 71	93	11	10
TD NiCr <sup>c, d</sup>	F	290	42	105	35	5.0	324	47	107	39	5.6	76	11	0.1	0.1	6	5
												<sup>e</sup> <sub>34</sub>	<sup>e</sup> <sub>5</sub>	<sup>e</sup> <sub>1268</sub>	---		
IN 713C <sup>c</sup>	E	814	118	109	103	14.9	1014	147	108	128	18.6	145	21	75, 54	64	12	22
Mar-M 509	G	296	43	80	33	4.9	621	90	105	70	10.2	103	15	151, 132	141	14	22
NX 188	G	724	105	85	---	----	903	131	101	---	----	97	14	118, 141	130	4	2
NASA VI-A	G	910	132	96	104	15.1	1117	162	102	127	18.5	205	29.8	72, 76	74	6	7
NASA WAZ-20	G	710	103	105	78	11.5	745	108	99	83	12.1	124	18	113, 48	81	4	11
René 80	G	758	110	110	93	13.5	1076	156	101	131	19.1	145	21	110, 127	118	11	12
IN 738 <sup>c</sup>	G	793	115	100	98	14.2	1014	147	105	125	18.1	138	20	23, 22	22	9	13
RBH <sup>f</sup>	---	312	45	---	36	5.1	504	73	---	58	8.3	103	15	-----	---	23	44
Mar-M 302	E	696	101	180	75	11.0	807	117	115	87	12.7	97	14	69, 95	82	3	8
U 700 cast	E	745	108	---	94	13.7	1020	148	114	129	18.7	124	18	121, 118	120	16	22
WI 52	E	579	84	168	65	9.5	765	111	126	86	12.5	90	13	158, 153	156	7	15
IN 100	E	793	115	92	102	14.8	965	140	90	125	18.1	172	25	94, 70	82	13	16
Mar-M 200	E	855	124	102	100	14.7	1000	145	107	117	17.2	179	26	114, 73	94	5	10
U 700 wrought	E	758	110	92	96	13.9	986	143	95	125	18.1	110	16	141, 133	137	30	32
M 22 <sup>c</sup>	E	958	139	124	111	16.1	1055	153	116	122	17.7	200	29	7.5, 11	9.3	8	4

<sup>a</sup> Average of duplicate tests.

<sup>b</sup> Nominal data (Specimens of heat used for thermal fatigue tests not available).

<sup>c</sup> Significantly lower rupture strength than nominal.

<sup>d</sup> Nominal data for 0.51-millimeter- (0.02-in.-) thick sheet.

<sup>e</sup> Supplementary test.

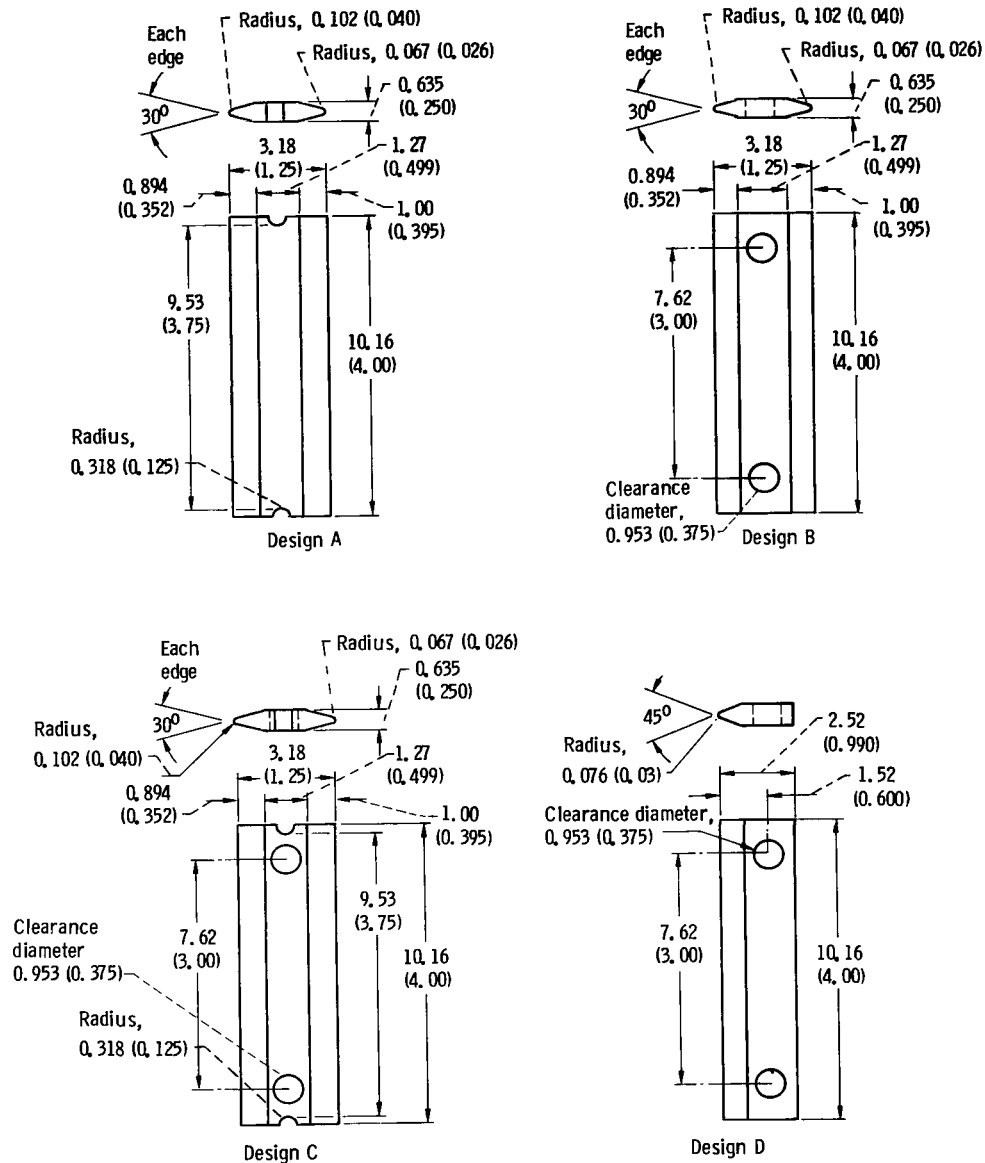
<sup>f</sup> Data for Haynes 1002 alloy which is similar to RBH (Specimens of heat used for thermal fatigue tests not available.).

TABLE V. - CYCLES TO CRACK INITIATION  
[DS indicates that the alloy was cast with a directionally solidified grain structure.]

Alloy	Bed temperatures <sup>a</sup>			
	1088° and 316° C (1990° and 600° F)		1129° and 357° C (2065° and 675° F)	
	Cycles	Specimen design (fig. 1(a))	Cycles	Specimen design (fig. 1(a))
NASA TAZ-8A + RT-XP coat	12 500	B		
Mar-M 200 DS + NiCrAlY overlay	4 500	C		
	8 500	C		
NASA TAZ-8A DS + NiCrAlY overlay	4 500	B		
	6 500	B		
NX 188 DS + RT-1A coat	5 100	B	>6100	B
	5 100	B		
NASA TAZ-8A DS	4 350	B	1200	B
	4 350	B		
	6 500	B		
NX 188 DS	4 350	B	5125	B
	4 350	B		
Mar-M 200 DS	1 250	C	1200	C
	1 750	C		
	4 700	A		
IN 100 DS + Jocoat	2 400	A	1950	C
IN 100 DS	2 400	A	1200	C
NASA WAZ-20 DS + Jocoat	1 750	B	1350	B
	1 750	B		
B 1900 + Hf + Jocoat	585	B	1550	B
	2 375	B		
B 1900 + Jocoat	1 190	A	1050	C
			>1200	C
NASA TAZ-8A	600	A	450	C
	800	C		
NX 188 + RT-1A coat	300	B	200	B
	800	B		
X 40	600	A	150	C
B 1900	400	A		
IN 162	400	A		
IN 100 + Jocoat	<sup>b</sup> 400	A	38	C
TD NiCr	250	A	13	C
IN 713C	250	A		
Mar-M 509	238	B	<sup>b</sup> 150	B
NX 188	100	B	50	B
	238	B		
NASA VI-A	138	B	<sup>b</sup> 38	B
NASA WAZ-20 + Jocoat	100	B	13	B
	138	B		
René 80	100	B	50	B
IN 738	100	B	50	B
RBH	100	B	50	B
Mar-M 302	75	A		
U 700 cast	75	A		
WI 52	75	A		
IN 100	38	A		
Mar-M 200 + Jocoat	25	C	<sup>b</sup> 13	C
Mar-M 200	13	A		
U 700 wrought	13	A		
M 22	13	A		

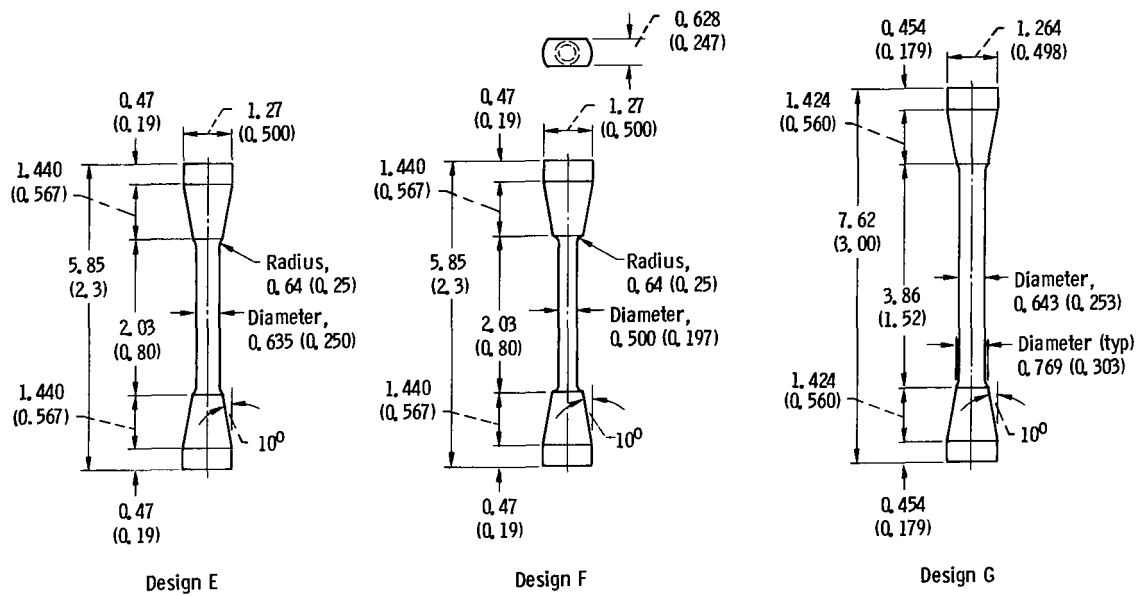
<sup>a</sup>3-minute immersion in both heating and cooling fluidized beds.

<sup>b</sup>1.02-millimeter (0.040-in.) radius edge failure.



(a) Thermal fatigue and oxidation specimens.

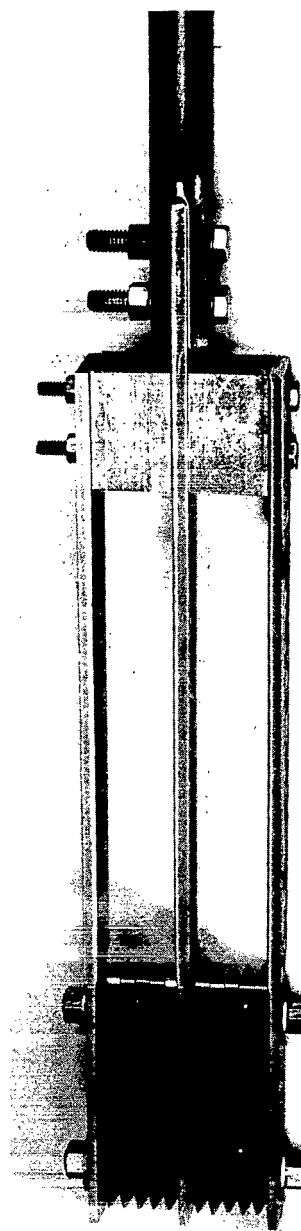
Figure 1. - Geometry of test specimens. (All dimensions in cm (in.) unless indicated otherwise.)



(b) Uniaxial specimens.  
Figure 1. - Concluded.



(a) Specimens with grooves  
(design A).



(b) Specimens with holes  
(designs B and C).

Figure 2. - Specimen holding fixture.

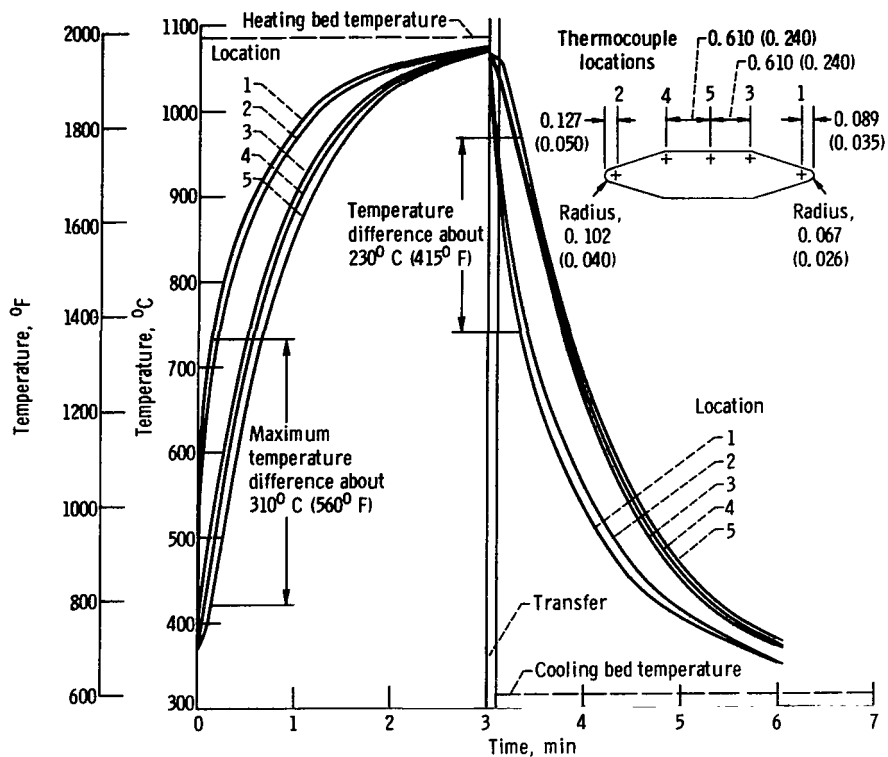
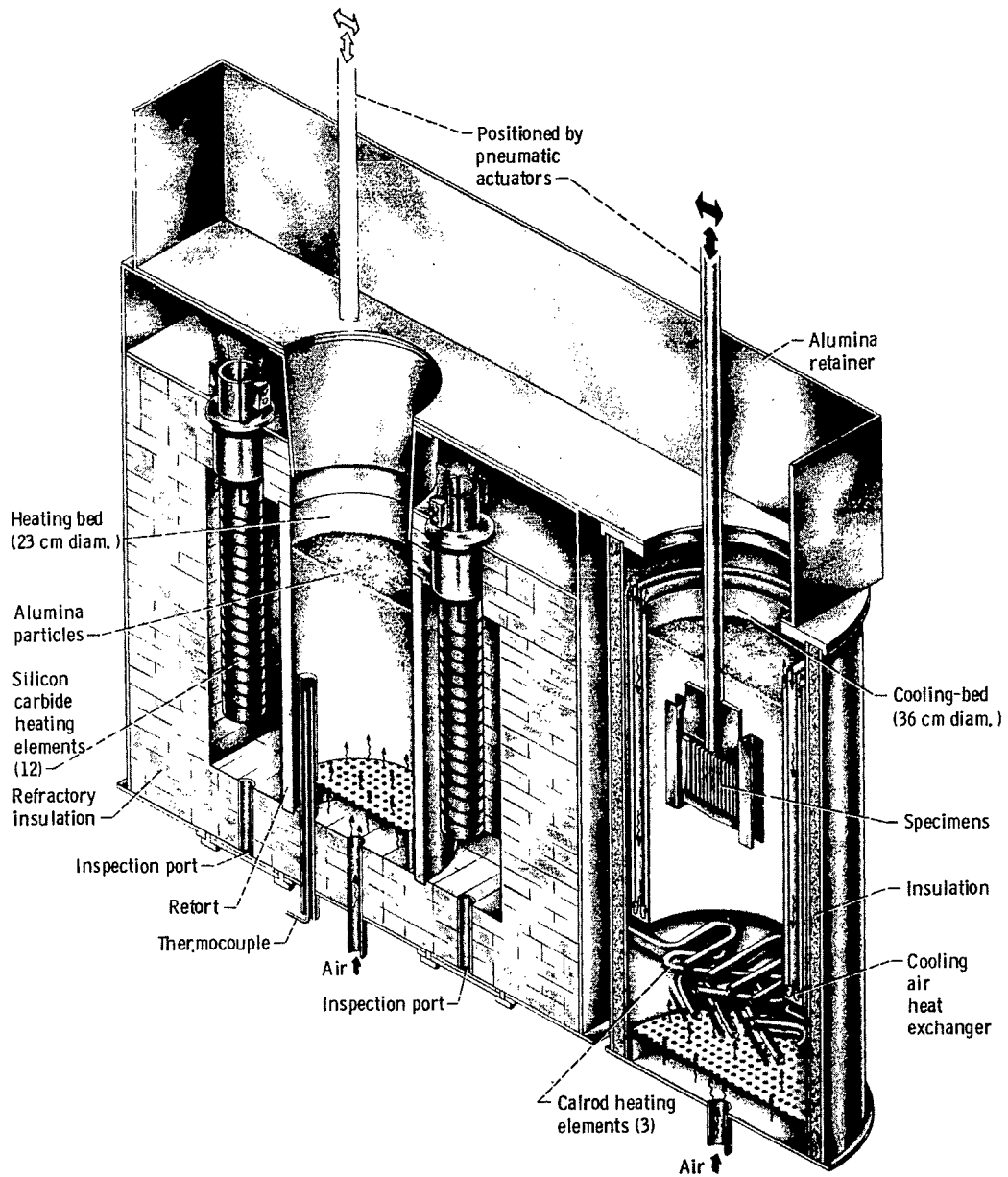


Figure 3. - Thermocouple locations and typical transient temperature of specimen tested in fluidized beds (directionally solidified NASA TAZ-8A alloy at bed temperatures of 1088° and 316° C (1990° and 600° F)). (All dimensions in cm (in.).)





CD-11823-34

Figure 4. - Fluidized bed test facility.

CS-73743

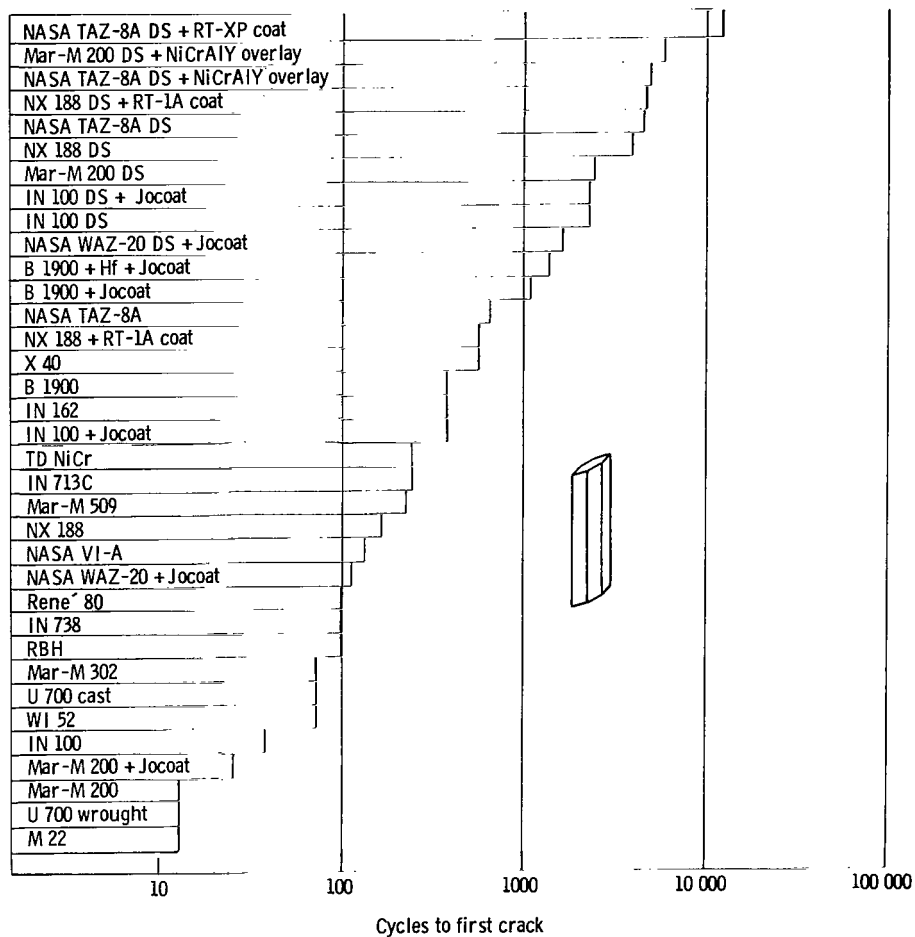


Figure 5. - Comparative thermal fatigue resistance. (Bed temperatures, 1088° and 316° C (1990° and 600° F) with a 3-minute immersion in each bed.)

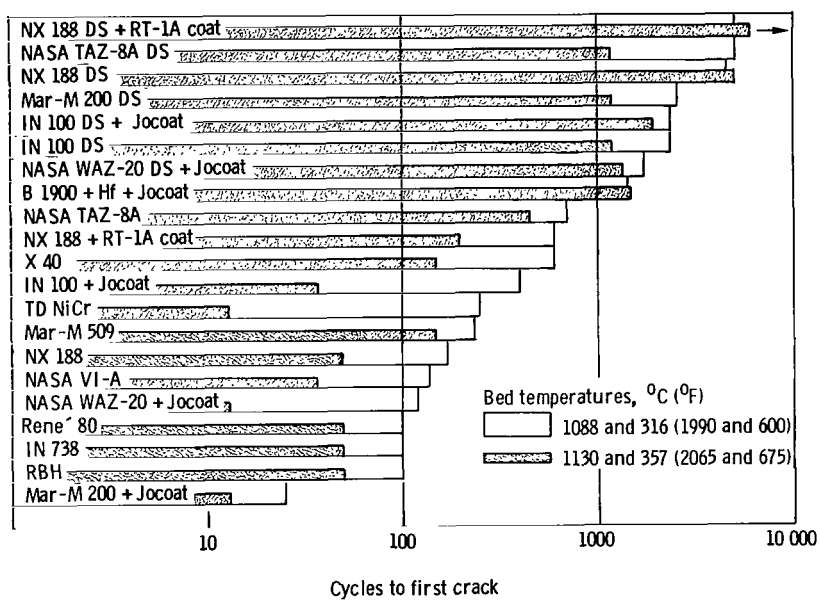


Figure 6. - Comparison of thermal fatigue resistance for alloys tested at both bed temperature conditions and alternately heated for 3 minutes and cooled for 3 minutes.

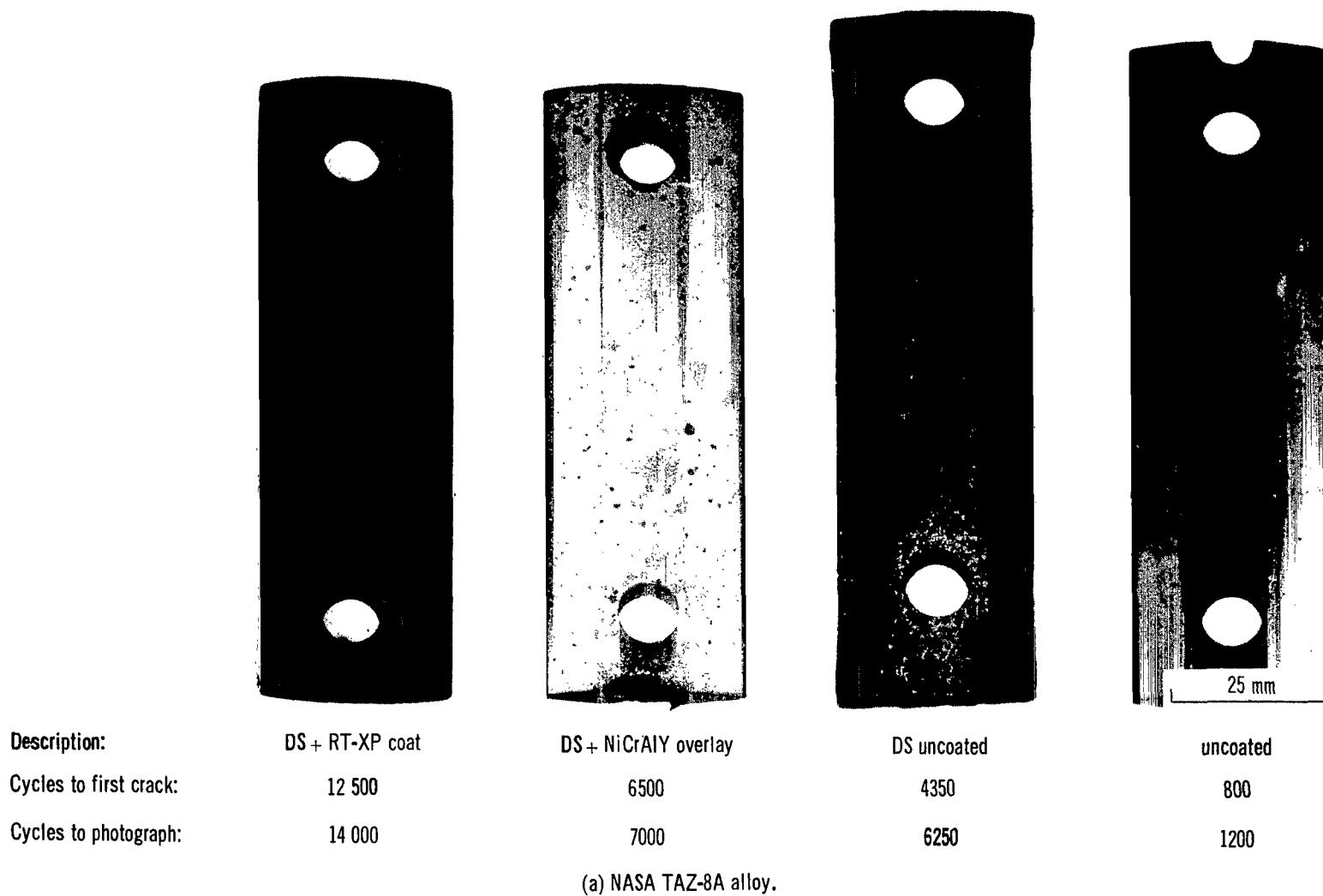
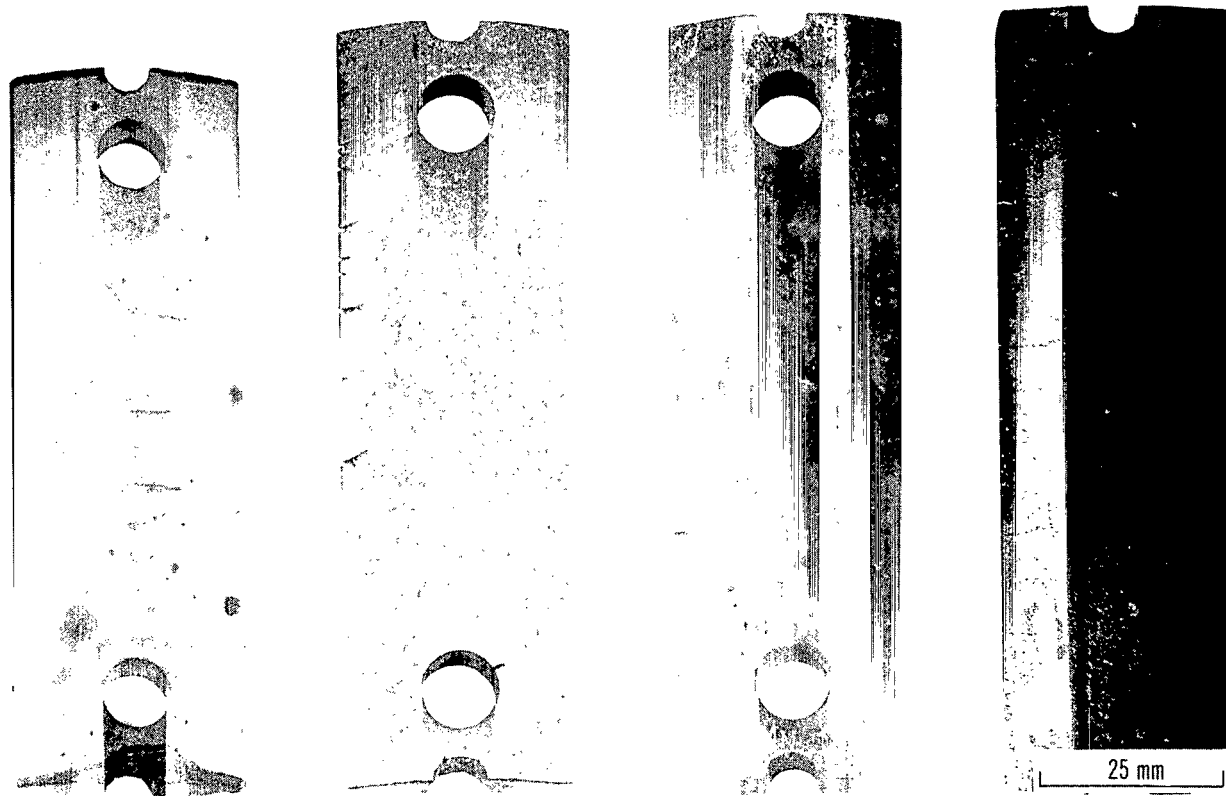


Figure 7. - Thermal fatigue specimens after testing at bed temperatures of 1088° and 316° C (1990° and 600° F).



Description:	DS + RT-1A coat	DS uncoated	+ RT-1A coat	Uncoated
Cycles to first crack:	5100	4350	800	100
Cycles to photograph:	6250	6250	1200	500

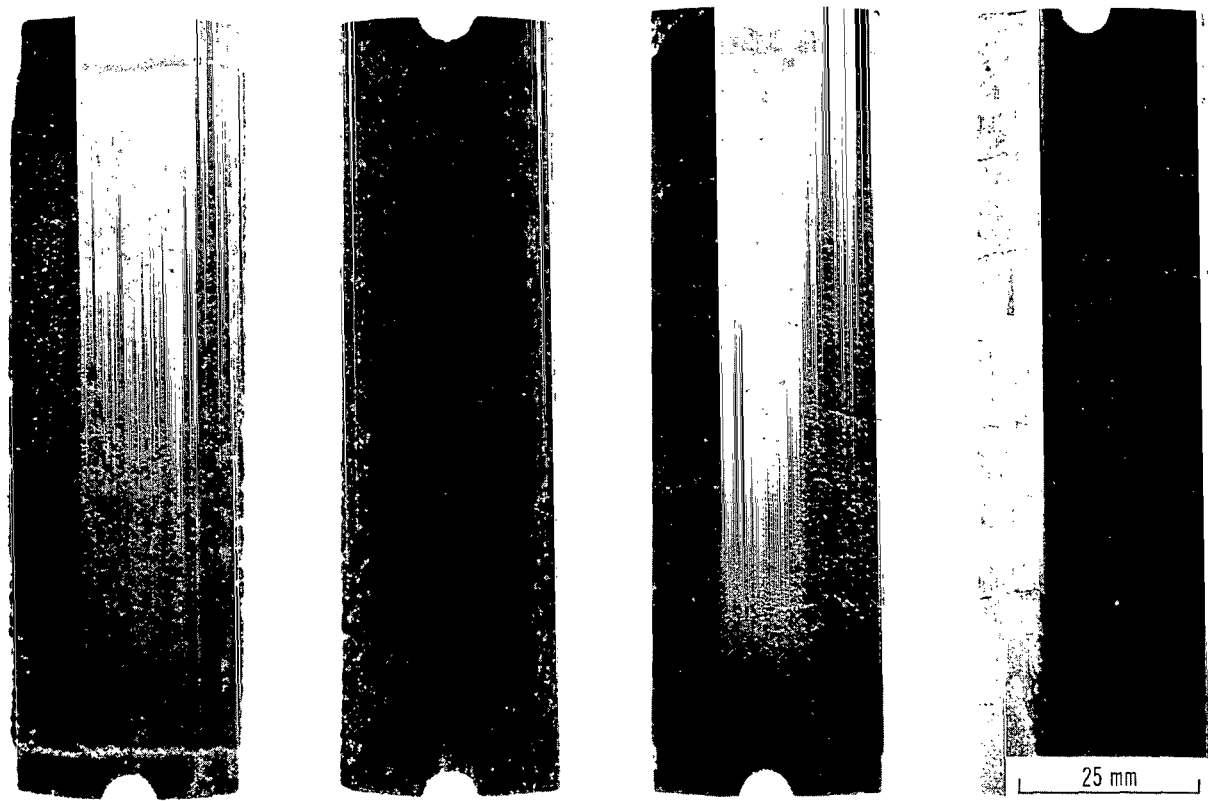
(b) NX 188 alloy.  
Figure 7. - Continued.



Description:	DS + NiCrAlY overlay	DS uncoated	+Jocoat	Uncoated
Cycles to first crack:	8 500	1750	25	13
Cycles to photograph:	10 000	4000	470	700

(c) Mar-M 200 alloy.

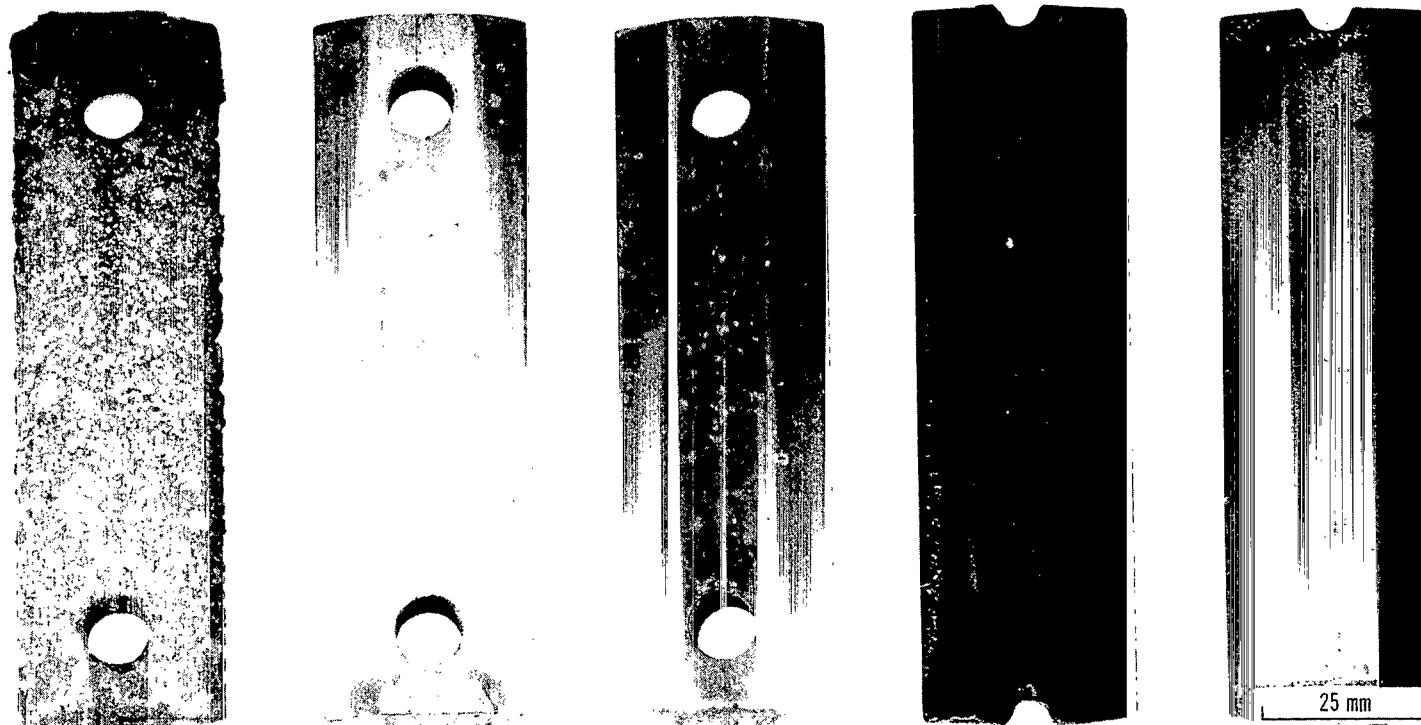
Figure 7. - Continued.



Description	DS + Jocoat	DS uncoated	+ Jocoat	Uncoated
Cycles to first crack:	2400	2400	400	38
Cycles to photograph:	5000	5000	2000	700

(d) IN 100 alloy.

Figure 7. - Continued.



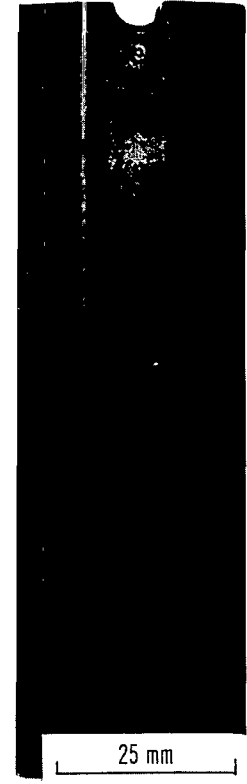
Description:	DS+ Jocoat	+ Jocoat	Hf modified + Jocoat	+ Jocoat	Uncoated
Cycles to first crack:	1750	138	585	1190	400
Cycles to photograph:	5500	700	1200	4400	2000

(e) NASA WAZ-20 alloy.

(f) B 1900 alloy.

Figure 7. - Continued.

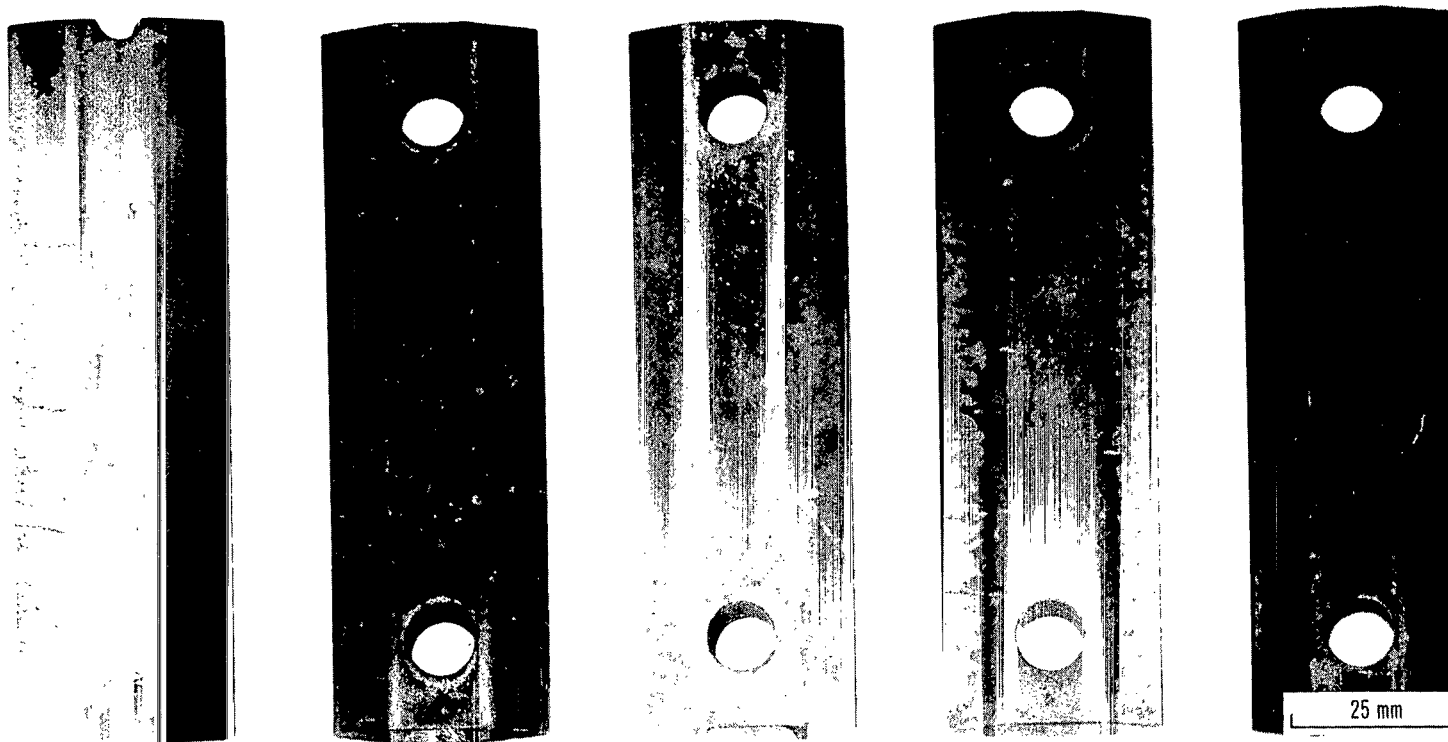




Description:	RBH	Mar-M 302	WI 52	M 22
Cycles to first crack:	100	75	75	13
Cycles to photograph:	500	700	700	700

(g) Other alloys.

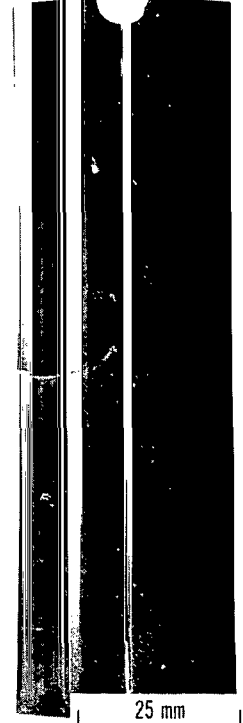
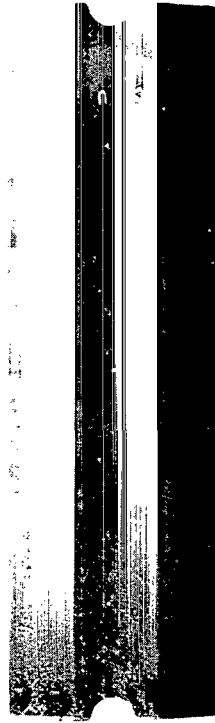
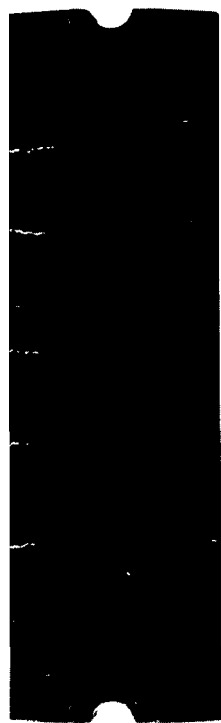
Figure 7. - Continued.



Description:	IN 713C	Mar-M 509	NASA VI-A	Rene 80	IN 738
Cycles to first crack:	250	238	138	100	100
Cycles to photograph:	700	700	700	500	500

(g) Continued. Other alloys.

Figure 7. - Continued.



Description:	U 700 cast	U 700 wrought	X 40	IN 162	TD NiCr
Cycles to first crack:	75	13	600	400	250
Cycles to photograph:	700	700	2000	3100	700

(g) Concluded. Other alloys.

Figure 7. - Concluded.

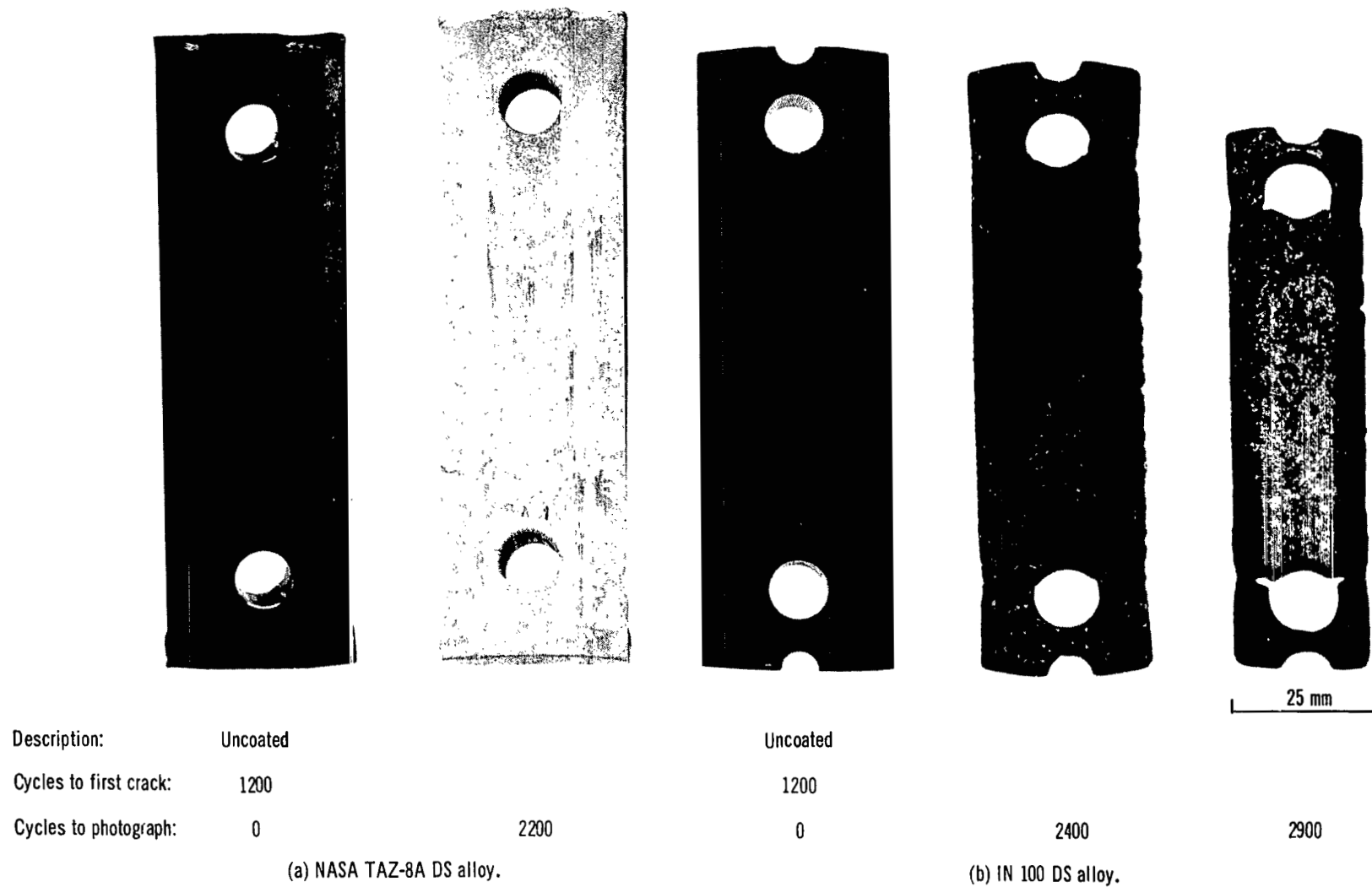
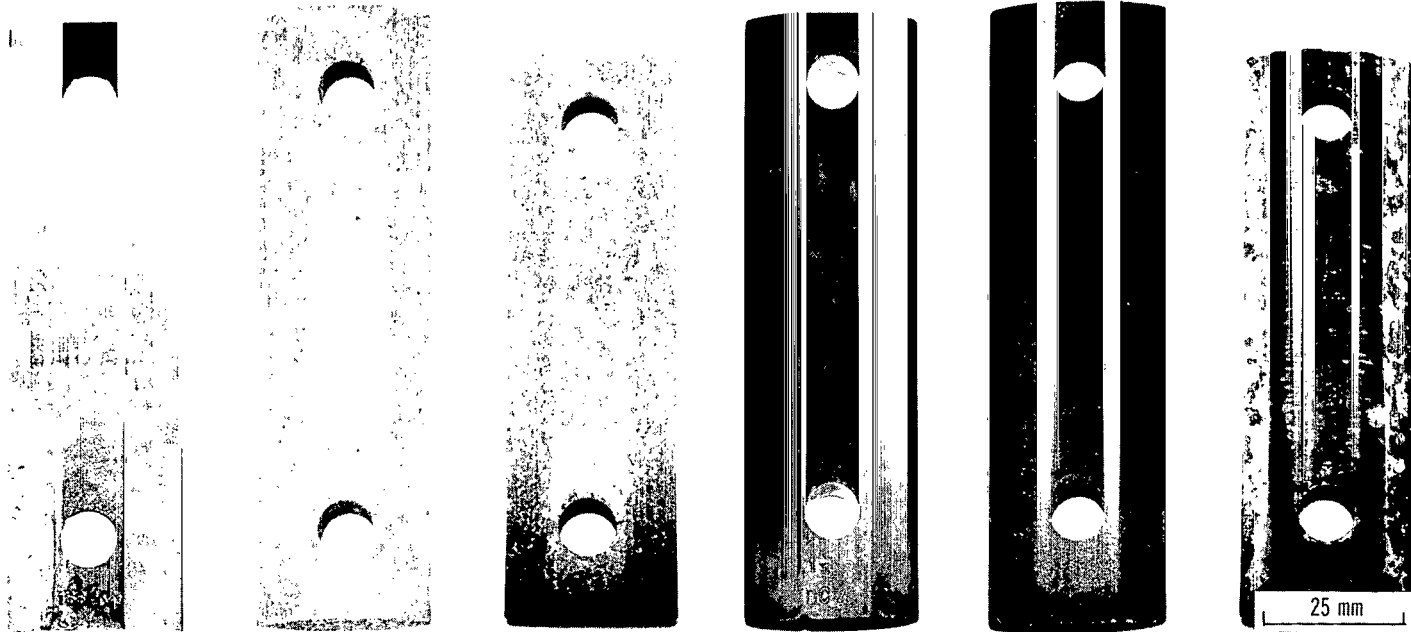


Figure 8. - Directionally solidified thermal fatigue specimens before and after testing at bed temperatures of 1130° and 357° C (2065° and 675° F).



Description: Uncoated

Cycles to first crack: 5125

Cycles to photograph: 0

2000

6500

+ RT-1A coat

> 6100

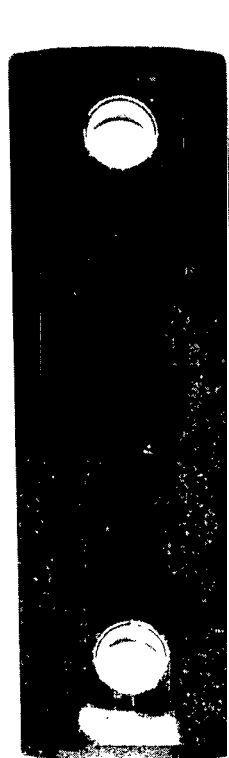
0

1600

6100

(c) NX 188 DS alloy.

Figure 8. - Continued.



Description: + Jocoat

Cycles to first crack: 1350

Cycles to photograph: 0

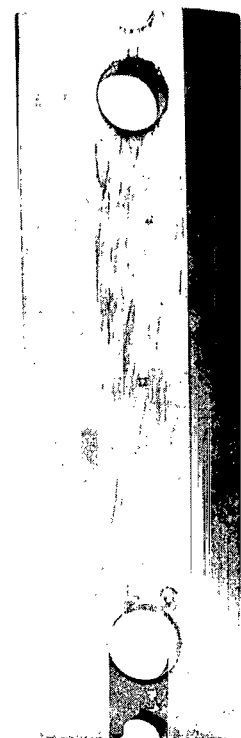


1600

(d) NASA WAZ-20 DS alloy.



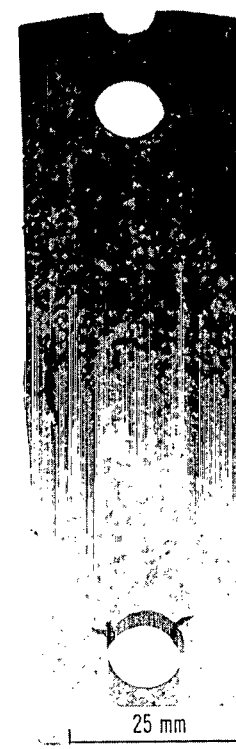
6100



Uncoated

1200

0



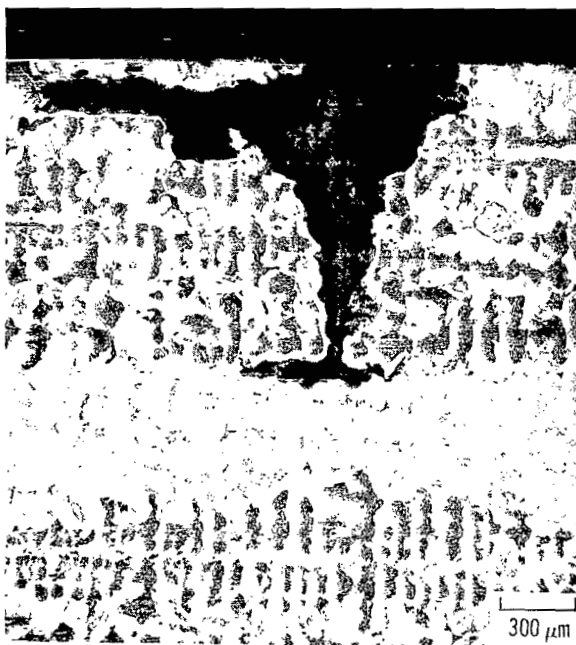
2400

(e) Mar-M 200 DS alloy.

Figure 8. - Concluded.

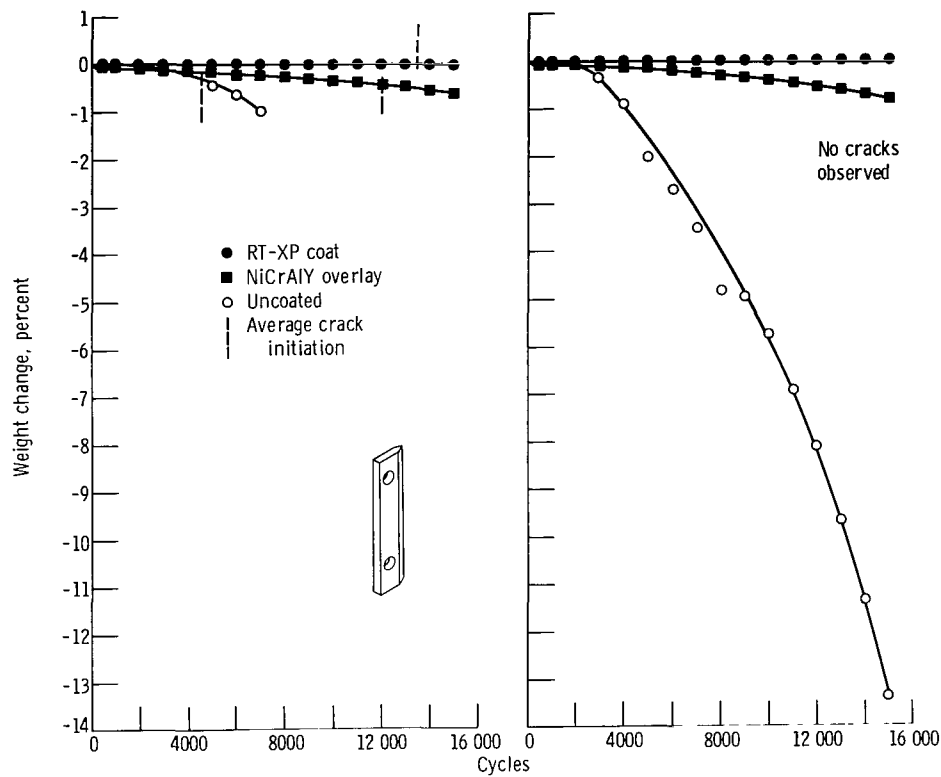


(a) Unetched.



(b) Etched.

Figure 9. - Photomicrographs of crack in directionally solidified NASA WAZ-20 + Jocoat after 5500 fluidized bed cycles at bed temperatures of 1130° and 357° C (2065° and 675° F) (ref. 9); X35.



(a) Random polycrystalline. (b) Directionally solidified polycrystalline.

Figure 10. - Weight change for NASA TAZ-8A. Immersion time in each bed was 3 minutes with bed temperatures at 1088° and 316° C (1990° and 600° F).

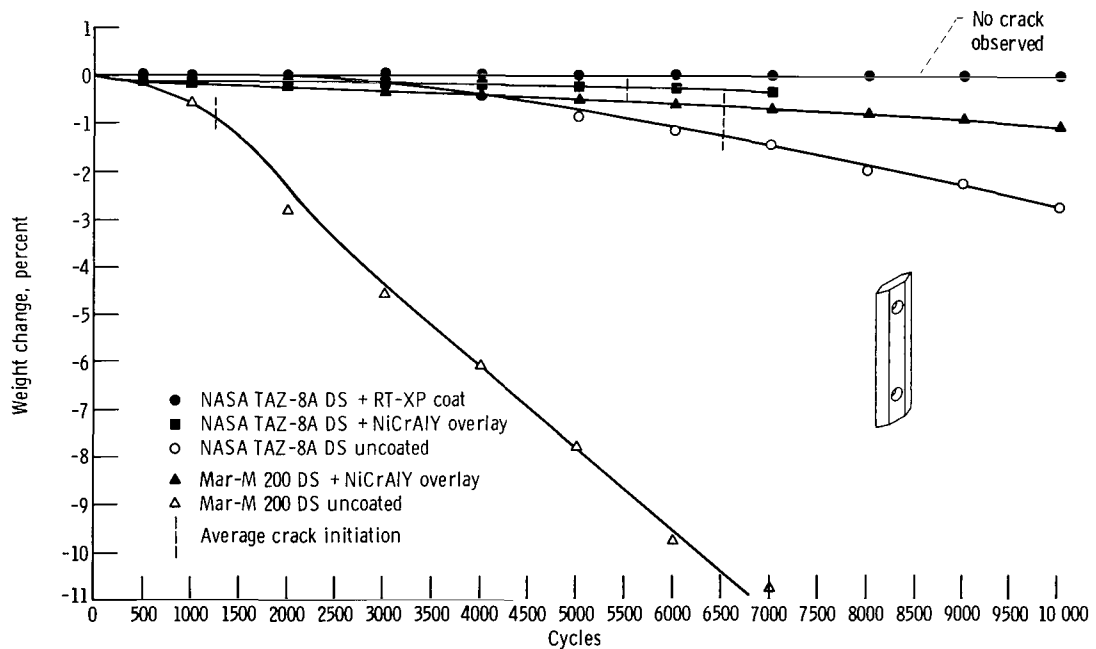


Figure 11. - Weight change for directionally solidified NASA TAZ-8A and Mar-M 200 alloys. Immersion time in each bed was 3 minutes with bed temperatures at 1088° and 316° C (1990° and 600° F).





991 001 C1 U D 751010 S00903DS  
DEPT OF THE AIR FORCE  
AF WEAPONS LABORATORY  
ATTN: TECHNICAL LIBRARY (SUL)  
KIRTLAND AFB NM 87117

POSTMASTER: If Undeliverable (Section 158  
Postal Manual) Do Not Return

*"The aeronautical and space activities of the United States shall be conducted so as to contribute . . . to the expansion of human knowledge of phenomena in the atmosphere and space. The Administration shall provide for the widest practicable and appropriate dissemination of information concerning its activities and the results thereof."*

—NATIONAL AERONAUTICS AND SPACE ACT OF 1958

## NASA SCIENTIFIC AND TECHNICAL PUBLICATIONS

**TECHNICAL REPORTS:** Scientific and technical information considered important, complete, and a lasting contribution to existing knowledge.

**TECHNICAL NOTES:** Information less broad in scope but nevertheless of importance as a contribution to existing knowledge.

**TECHNICAL MEMORANDUMS:** Information receiving limited distribution because of preliminary data, security classification, or other reasons. Also includes conference proceedings with either limited or unlimited distribution.

**CONTRACTOR REPORTS:** Scientific and technical information generated under a NASA contract or grant and considered an important contribution to existing knowledge.

**TECHNICAL TRANSLATIONS:** Information published in a foreign language considered to merit NASA distribution in English.

**SPECIAL PUBLICATIONS:** Information derived from or of value to NASA activities. Publications include final reports of major projects, monographs, data compilations, handbooks, sourcebooks, and special bibliographies.

**TECHNOLOGY UTILIZATION PUBLICATIONS:** Information on technology used by NASA that may be of particular interest in commercial and other non-aerospace applications. Publications include Tech Briefs, Technology Utilization Reports and Technology Surveys.

*Details on the availability of these publications may be obtained from:*

**SCIENTIFIC AND TECHNICAL INFORMATION OFFICE  
NATIONAL AERONAUTICS AND SPACE ADMINISTRATION  
Washington, D.C. 20546**